First-Principles Study of Electron Linewidths in Graphene

Cheol-Hwan Park[1,2], Feliciano Giustino[1,2,3], Catalin D. Spataru[4], Marvin L. Cohen[1,2], and Steven G. Louie[1,2*]
[1] *Department of Physics, University of California at Berkeley, Berkeley, California 94720 USA*
[2] *Materials Sciences Division, Lawrence Berkeley National Laboratory, Berkeley, California 94720 USA*
[3] *Department of Materials, University of Oxford, Oxford, OX1 3PH, United Kingdom*
[4] *Sandia National Laboratories, Livermore, California 94551 USA*

(Dated: February 20, 2009)

We present first-principles calculations of the linewidths of low-energy quasiparticles in n-doped graphene arising from both the electron-electron and the electron-phonon interactions. The contribution to the electron linewidth arising from the electron-electron interactions vary significantly with wavevector at fixed energy; in contrast, the electron-phonon contribution is virtually wavevector-independent. These two contributions are comparable in magnitude at a binding energy of ~ 0.2 eV, corresponding to the optical phonon energy. The calculated linewidths, with both electron-electron and electron-phonon interactions included, explain to a large extent the linewidths seen in recent photoemission experiments.

Graphene [1, 2, 3], a single layer of carbon atoms in a hexagonal honeycomb structure, is a unique system whose carrier dynamics can be described by a massless Dirac equation [4]. Within the quasiparticle picture, carriers in graphene exhibit a linear energy dispersion relation and chiral behavior resulting in a half-integer quantum Hall effect [1, 2], absence of backscattering [5, 6], Klein tunneling [7], and novel phenomena such as electron supercollimation in superlattices [8, 9, 10].

Graphene is considered a promising candidate for electronic and spintronic devices [11]. For these applications it is important to understand the effects of many-body interactions on carrier dynamics. In particular, the scattering rate of charge carriers, manifested in their linewidths, affects the transport properties of actual devices.

The scattering of charge carriers in solids can arise from several different mechanisms, among which electron-hole pair generation, electron-plasmon interaction, and electron-phonon (e-ph) interaction are generally important. Scattering by impurities, defects and interactions with the substrate also affects the carrier dynamics. The contribution to the electron linewidths arising from the e-ph interaction has been studied with first-principles calculations [12, 13] and through the use of analytical and numerical calculations based on the massless Dirac equation [14, 15]. The linewidth contribution originating from electron-electron (e-e) interactions, which includes both the electron-hole pair generation process and the electron-plasmon interaction, has only been studied within the massless Dirac equation formalism [16, 17, 18].

A recent angle-resolved photoemission experiment on n-doped graphene epitaxially grown on silicon carbide (SiC) [19] has stimulated experimental [20, 21, 22] and theoretical [12, 14, 15, 16, 17, 18] studies on this topic. In Ref. 19, the width of the momentum distribution curve (MDC) from photoemission data is presented. The MDC of the graphene photoemission spectra is observed to resemble a simple Lorentzian whose width may be interpreted to be directly proportional to the scattering rate [19].

We draw the attention to the well-known controversy in the different interpretations of the angle-resolved photoemission spectra of graphene. It is claimed in Ref. 19 that the spectral features can entirely be understood from many-body effects, including both e-e and e-ph interactions, in graphene. On the other hand, in Ref. 20, it is argued that many of those features are dominated by an energy gap of 0.2$\sim$0.3 eV, which opens up at the Dirac point energy ($E_{\rm D}$) because of interactions between graphene and the reconstructed surface of SiC. This important problem in understanding the quasiparticle spectra of graphene (which also have implications in graphene-based electronics applications) has led to numerous additional experiments directly or indirectly addressing this discrepancy [23, 24, 25, 26, 27, 28]. On the theoretical side, several density functional theory calculations on the effect of substrates without considering many-body effects, along the line of Ref. 20, have been performed [29, 30, 31]. On the other hand, first-principles calculations on the effects of both e-e and e-ph interactions, along the line of Ref. 19, have been lacking up to now.

In this paper, to fill in this missing part, we present *ab initio* calculations of the electron linewidth in n-doped graphene arising from e-e interactions employing the GW approximation [32, 33, 34]. In addition, we calculate the electron linewidth originating from the e-ph interaction following the method in Refs. 12, 35 and 36. Combining both contributions, we provide a comprehensive view of the scattering rate originating from many-body effects. Our calculation indicates that the linewidth arising from e-e interactions is highly anisotropic. This is in contrast to the insensitivity to wavevector of the phonon-induced electron linewidth shown in Ref. 13. The calculated linewidth arising from e-e interaction becomes comparable to that arising from e-ph interaction at a binding energy of $\sim$ 0.2 eV (i. e. , the optical phonon energy). The combination of the two contributions accounts for

*Electronic address: sglouie@berkeley.edu

most of the measured linewidth over the 0 eV $\sim$ 2.5 eV binding energy range.

The electronic eigenstates $|n\mathbf{k}\rangle$ of graphene are obtained with *ab initio* pseudopotential density-functional calculations [37] in the local density approximation (LDA) [38, 39] in a supercell geometry. Electronic wavefunctions in a $72 \times 72 \times 1$ $\mathbf{k}$-point grid are expanded in a plane-waves basis [40] with a kinetic energy cutoff of 60 Ry. The core-valence interaction is treated by means of norm-conserving pseudopotentials [41]. Graphene layers between adjacent supercells are separated by 8.0 Å and the Coulomb interaction is truncated to prevent spurious interaction between periodic replicas [42]. Increasing the interlayer distance to 16.0 Å makes virtually no difference in the calculated electron self-energy. Doped graphene is modeled by an extra electron density with a neutralizing background.

We calculate the imaginary part of the electron self-energy induced by the e-e interaction within the GW approximation [32, 34]. The frequency dependent dielectric matrices $\epsilon_{\mathbf{G},\mathbf{G}'}(\mathbf{q},\omega)$ are calculated within the random phase approximation using the LDA wavefunctions on a regular grid of ω with spacing $\Delta\omega$ =0.125 eV [43], and a linear interpolation is performed to obtain the dielectric matrices for energies in between the grid points. In the calculation of the polarizability, for numerical convergence, an imaginary component of magnitude $\Delta\omega$ of 0.125 eV as above is introduced in the energy denominator. Convergence tests showed that the dimension of $\epsilon_{\mathbf{G},\mathbf{G}'}$ may be truncated at a kinetic energy cutoff of $\hbar^2 G^2/2m$ =12 Ry. To take into account the screening of the SiC substrate, we have renormalized the bare Coulomb interaction by an effective background dielectric constant of $\varepsilon_{\rm b} = (1+\varepsilon_{\rm SiC})/2 = 3.8$ [16, 17, 18, 19], where $\varepsilon_{\rm SiC}(= 6.6)$ is the optical dielectric constant of SiC [44, 45].

Figure 1 shows the calculated imaginary part $\mathrm{Im}\,\Sigma^{e-e}_{n\mathbf{k}}(\varepsilon_{n\mathbf{k}}) = \langle n\mathbf{k}|\,\mathrm{Im}\,\Sigma^{e-e}(\mathbf{r},\mathbf{r}',\varepsilon_{n\mathbf{k}})\,|n\mathbf{k}\rangle$ of the electron self-energy arising from the e-e interaction with ω set at the LDA eigenvalue $\varepsilon_{n\mathbf{k}}$. The Fermi level $E_{\rm F}$ (= 0) is taken to be 1 eV above $E_{\rm D}$. In Fig. 1(a), $\mathrm{Im}\,\Sigma^{e-e}_{n\mathbf{k}}(\varepsilon_{n\mathbf{k}})$ for graphene without including substrate screening, appropriate for suspended graphene [46, 47], is plotted along the KΓ direction. Generally, the self-energy increases with increasing $|\varepsilon_{n\mathbf{k}}|$ as measured from $E_{\rm F}$. A notable feature is the peak around $\varepsilon_{n\mathbf{k}} = -1.5$ eV. To find the origin of this peak, we have decomposed the total electron self-energy into the contributions arising from transitions into the upper linear bands (above $E_{\rm D}$) and the lower linear bands (below $E_{\rm D}$). The former involves electron-plasmon interaction [16]. The peak structure comes from scattering processes of electrons into the upper linear bands, whereas those scattering processes into the lower linear bands result in a monotonic increase in the electron linewidth. When the background dielectric constant $\varepsilon_{\rm b}$ is changed from 1 to 3.8 [Fig. 1(b)], the position of this peak shifts toward lower-binding energy by $\sim$ 0.3 eV, reflecting a decrease of the plasmon energy in graphene

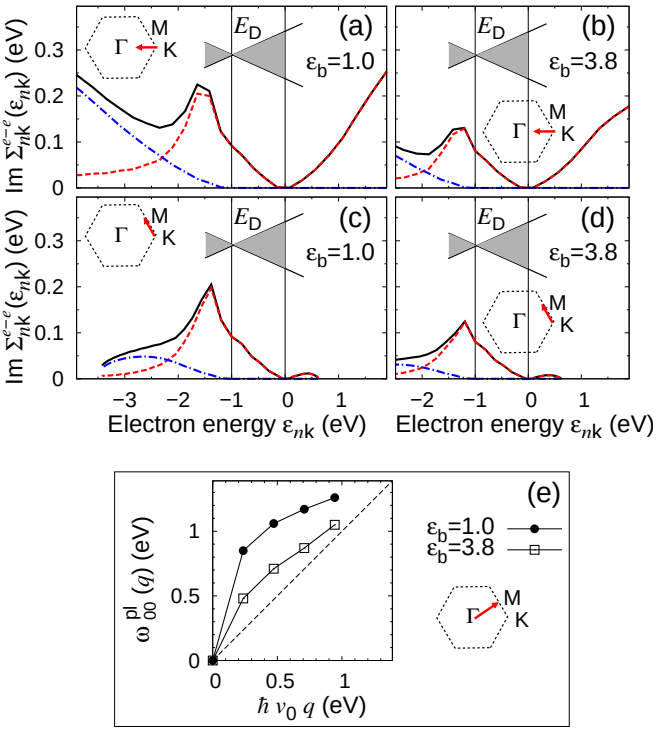

FIG. 1: (color online). (a)-(d): Calculated imaginary part of the electron self-energy arising from the e-e interaction, $\mathrm{Im}\,\Sigma^{e-e}_{n\mathbf{k}}(\varepsilon_{n\mathbf{k}})$, versus the LDA energy $\varepsilon_{n\mathbf{k}}$ (solid black lines) in n-doped graphene. The Dirac point energy $E_{\rm D}$ is 1.0 eV below the Fermi level. The contributions to $\mathrm{Im}\,\Sigma^{e-e}_{n\mathbf{k}}(\varepsilon_{n\mathbf{k}})$ coming from electronic transitions to the upper linear bands and to the lower linear bands are shown as dashed red lines and dash-dotted blue lines, respectively. The self-energy is evaluated along the reciprocal space segments shown in the insets. (a) and (c) are results for suspended graphene with a background dielectric constant of $\varepsilon_{\rm b} = 1.0$, whereas (b) and (d) are results for graphene with a background dielectric constant of $\varepsilon_{\rm b} = (1+\varepsilon_{\rm SiC})/2 = 3.8$. The Fermi level and $E_{\rm D}$ are indicated by vertical lines. (e): Calculated plasmon energy dispersion relation $\omega^{\rm pl}_{00}(\mathbf{q})$, given by $\epsilon_{\mathbf{G}=0,\mathbf{G}'=0}[\mathbf{q},\omega^{\rm pl}_{00}(\mathbf{q})] = 0$, versus $\hbar v_0|\mathbf{q}|$ along the ΓM direction. The solid lines are guides to the eye and the dashed line corresponds to $\omega(q) = \hbar v_0 q$.

[Fig. 1(e)] [48, 49]. The height of the peak is further suppressed. At low energy ($|\varepsilon_{n\mathbf{k}}| < 1.0$ eV), the imaginary part of the self-energy is however not sensitive to the choice of $\varepsilon_{\rm b}$.

Comparing Figs. 1(a) and 1(b) with Figs. 1(c) and 1(d) shows that the electron self-energy arising from the e-e interaction calculated along the KM direction is very different from that along the KΓ direction. Below -1.5 eV, $\mathrm{Im}\,\Sigma^{e-e}_{n\mathbf{k}}(\varepsilon_{n\mathbf{k}})$ along K→M decreases with increasing $|\varepsilon_{n\mathbf{k}}|$, and it almost vanishes at the M point. This strong $\mathbf{k}$ anisotropy in the e-e contribution to the imaginary part of the self-energy is a band structure effect, and is absent in calculations based on the massless Dirac equation. This behavior is in contrast with the wavevector insensitivity of the phonon-induced electron self-energy [13] (Fig. 2). The calculated real part [50]

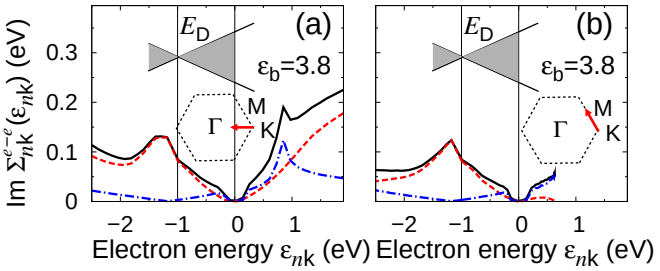

FIG. 2: (color online). Calculated Im $\Sigma_{n\mathbf{k}}(\varepsilon_{n\mathbf{k}})$ versus the LDA energy eigenvalue $\varepsilon_{n\mathbf{k}}$ in n-doped graphene ($E_D = -1.0$ eV) on a model substrate ($\varepsilon_b = 3.8$). The total self-energy, the self-energy arising from the e-e interaction, and that arising from the e-ph interaction are shown in solid black, dashed red and dash-dotted blue lines, respectively. The self-energy is evaluated along the reciprocal space segments shown in the insets.

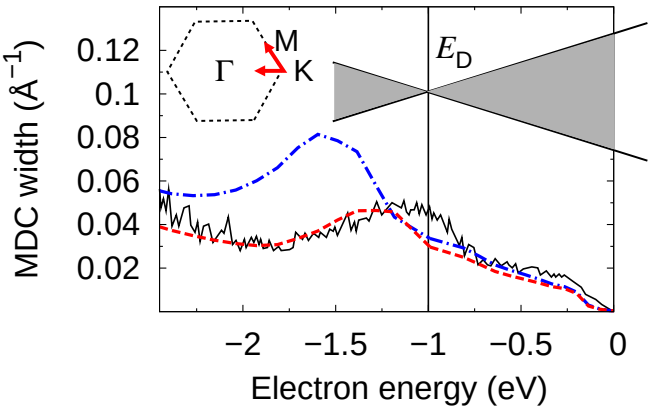

FIG. 3: (color online). MDC width versus binding energy in n-doped graphene ($E_D = -1.0$ eV). Calculated quantities for suspended graphene ($\varepsilon_b = 1.0$) and for graphene on a model substrate ($\varepsilon_b = 3.8$) are shown in dash-dotted blue and dashed red lines, respectively. The experimental result measured for sample corresponding to the highest level of doping in Fig. 3 of Ref. 19 are shown as the solid black line [54]. Both the experimental and the calculated results are along the KM and the KΓ direction of the Brillouin zone when the electron energy is above and below E_D, respectively.

and the imaginary part [34] of the electron self-energy in bulk graphite arising from the e-e interaction are also anisotropic, in line with the present findings.

Figures 2(a) and 2(b) show the electron self-energy in n-doped graphene ($E_D = -1.0$ eV) on a substrate (model with $\varepsilon_b = 3.8$) arising both from the e-e and the e-ph interaction. The Im $\Sigma_{n\mathbf{k}}(\varepsilon_{n\mathbf{k}})$ along the two different directions KΓ and KM are qualitatively different at high binding energy. This anisotropy is due to the e-e interaction, and not the e-ph interaction [13]. It is noted that the total linewidth along the KM direction is almost constant for binding energies in the range 1.7 to 3.5 eV. These anisotropic features should be observable in photoemission experiments.

The e-e and the e-ph interactions give comparable contributions to the imaginary part of the electron self-energy, especially within a few tenths of an eV from the Fermi level (Fig. 2). This behavior is peculiar to graphene. In most metals the e-ph contribution to the electron self-energy near E_F is generally dominant over the e-e contribution at energies comparable to the relevant phonon energy scale [51]. Similarly large Im $\Sigma_{n\mathbf{k}}(\varepsilon_{n\mathbf{k}})$ due to e-e interactions are obtained in the Dirac Hamiltonian calculations in Refs. 16 and 17 if the same background dielectric constant ε_b is used. Because of this peculiar aspects of graphene, an e-ph coupling strength λ extracted from measured data could be overestimated if the e-e interaction is neglected. This may explain why the e-ph coupling strength λ extracted from photoemission spectra [21] is larger than the theoretical calculations [13, 14], together with the effects of bare band curvature [13] and dopants.

We now compare the imaginary part of the electron self-energy obtained from our calculation with the MDC width obtained from measured photoemission spectra [19]. For a linear bare band energy dispersion, the spectral function at a fixed energy ω is a Lorentzian as a function of the wavevector measured from the **K** point [19]. Thus, the width of the MDC Δk at energy $\omega = \varepsilon_{n\mathbf{k}}$ can be identified as $\Delta k(\varepsilon_{n\mathbf{k}}) = 2\mathrm{Im}\,\Sigma_{n\mathbf{k}}(\varepsilon_{n\mathbf{k}})/\hbar v_0$ where v_0 is the LDA band velocity of low-energy charge carriers in graphene [12, 19]. (For the n-doped graphene with $E_D = -1.0$ eV, the bare band dispersion is, to a good approximation, linear in the energy range considered in Fig. 3.)

Figure 3 shows the calculated MDC width for suspended graphene ($\varepsilon_b = 1.0$) and for our model of graphene on SiC ($\varepsilon_b = 3.8$). The substrate screening affects the position and the strength of the peak arising from the electron-plasmon interaction, while the low-energy part is insensitive to the dielectric screening from the substrate. The calculated MDC width for graphene when substrate screening is accounted for is in agreement with the experimental data of Ref. 19 throughout the whole energy window shown in Fig. 3. However, the experimentally measured MDC width in a 0.4 eV energy window around E_D (=-1.0 eV) is larger than that from our calculation. This enhanced linewidth may possibly arise from the gap which opens up at E_D and midgap states originating from the interactions between graphene and SiC substrate with a carbon buffer layer [20, 29, 30, 31].

In conclusion, we have studied the electron linewidths of n-doped graphene including both the e-e and the e-ph interaction contributions, using first-principles calculations. The imaginary part of the electron self-energy arising from the e-e interaction is strongly anisotropic in **k**-space. We have shown that for graphene, unlike in conventional metals, the e-e contribution is comparable to the e-ph contribution at low binding-energy. Our calculation explains most of the scattering rate observed in a recent photoemission experiment [19]; however, near

the Dirac point energy, the calculated scattering rate is smaller than the measured one, suggesting the possibility of band gap opening and midgap states. These results contribute to the resolution of the important controversy introduced earlier in this paper and encourages further theoretical studies including both many-body interactions and substrate effects at an atomistic level. More generally, our first-principles calculations convincingly demonstrate that multiple many-body interactions ought to be considered on the same footing in order to achieve a quantitative and comprehensive interpretation of high-resolution angle-resolved photoemission spectra.

We thank A. Lanzara, J. L. McChesney, A. Bostwick, T. Ohta, E. Rotenberg, S. Ismail-Beigi, E. H. Hwang and J. D. Sau for fruitful discussions. This work was supported by NSF Grant No. DMR07-05941 and by the Director, Office of Science, Office of Basic Energy Sciences, Division of Materials Sciences and Engineering Division, U.S. Department of Energy under Contract No. DE-AC02-05CH11231. Sandia is a multiprogram laboratory operated by Sandia Corporation, a Lockheed Martin Company, for the United States Department of Energy under Contract No. DE-AC01-94-AL85000. Computational resources have been provided by NPACI and NERSC. The calculations were performed using the `PARATEC` [55], `BerkeleyGW` [56], `Quantum-Espresso` [57] and `Wannier` [58] packages.

[1] K. S. Novoselov *et al.*, Nature **438**, 197 (2005).
[2] Y. Zhang, J. W. Tan, H. L. Stormer, and P. Kim, Nature **438**, 201 (2005).
[3] C. Berger *et al.*, Science **312**, 1191 (2006).
[4] P. R. Wallace, Phys. Rev. **71**, 622 (1947).
[5] T. Ando and T. Nakanishi, J. Phys. Soc. Jpn. **67**, 1704 (1998).
[6] P. L. McEuen *et al.*, Phys. Rev. Lett. **83**, 5098 (1999).
[7] M. I. Katsnelson, K. S. Novoselov, and A. K. Geim, Nature Phys. **2**, 620 (2006).
[8] C.-H. Park *et al.*, Nature Phys. **4**, 213 (2008).
[9] C.-H. Park *et al.*, Nano Lett. **8**, 2920 (2008).
[10] C.-H. Park *et al.*, Phys. Rev. Lett. **101**, 126804 (2008).
[11] A. K. Geim and K. S. Novoselov, Nature Mater. **6**, 183 (2007).
[12] C.-H. Park, F. Giustino, M. L. Cohen, and S. G. Louie, Phys. Rev. Lett. **99**, 086804 (2007).
[13] C.-H. Park *et al.*, Phys. Rev. B **77**, 113410 (2008).
[14] M. Calandra and F. Mauri, Phys. Rev. B **76**, 205411 (2007).
[15] W.-K. Tse and S. D. Sarma, Phys. Rev. Lett. **99**, 236802 (2007).
[16] M. Polini *et al.*, Phys. Rev. B **77**, 081411 (2008).
[17] E. H. Hwang and S. D. Sarma, Phys. Rev. B **77**, 081412 (2008).
[18] E. H. Hwang, B. Y.-K. Hu, and S. D. Sarma, Phys. Rev. B **76**, 115434 (2007).
[19] A. Bostwick *et al.*, Nature Phys. **3**, 36 (2007).
[20] S. Y. Zhou, D. A. Siegel, A. V. Fedorov, and A. Lanzara, Nature Mater. **6**, 770 (2007).
[21] J. McChesney *et al.*, arXiv:0705.3264v1 .
[22] T. Ohta *et al.*, Phys. Rev. Lett. **98**, 206802 (2007).
[23] T. Ohta *et al.*, New J. Phys. **10**, 023034 (2008).
[24] A. Bostwick *et al.*, New J. Phys. **9**, 385 (2007).
[25] E. Rotenberg *et al.*, Nature Mater. **7**, 258 (2008).
[26] S. Y. Zhou *et al.*, Nature Mater. **7**, 259 (2008).
[27] S. Y. Zhou, D. A. Siegel, A. V. Fedorov, and A. Lanzara, Physica E **40**, 2642 (2008).
[28] S. Y. Zhou, D. A. Siegel, A. V. Fedorov, and A. Lanzara, Phys. Rev. Lett. **101**, 086402 (2008).
[29] S. Kim, J. Ihm, H. J. Choi, and Y.-W. Son, Phys. Rev. Lett. **100**, 176802 (2008).
[30] A. Mattausch and O. Pankratov, Phys. Rev. Lett. **99**, 076802 (2007).
[31] F. Varchon *et al.*, Phys. Rev. Lett. **99**, 126805 (2007).
[32] M. S. Hybertsen and S. G. Louie, Phys. Rev. B **34**, 5390 (1986).
[33] First-principles calculations of the electron velocity renormalization in graphene arising from *e*-*e* interaction have recently been performed [P. E. Trevisanutto *et al.*, Phys. Rev. Lett. **101**, 226405 (2008); C. Attaccalite, A. Grüeneis, T. Pichler, and A. Rubio, arXiv:0808.0786v1].
[34] C. D. Spataru *et al.*, Phys. Rev. Lett. **87**, 246405 (2001).
[35] C.-H. Park, F. Giustino, M. L. Cohen, and S. G. Louie, Nano Lett. **8**, 4229 (2008).
[36] F. Giustino, M. L. Cohen, and S. G. Louie, Phys. Rev. B **76**, 165108 (2007).
[37] *Conceptual Foundations of Materials: A Standard Model for Ground- and Excited-State Properties*, edited by S. G. Louie and M. L. Cohen (Elsevier, Amsterdam, 2006).
[38] D. M. Ceperley and B. J. Alder, Phys. Rev. Lett. **45**, 566 (1980).
[39] J. P. Perdew and A. Zunger, Phys. Rev. B **23**, 5048 (1981).
[40] J. Ihm, A. Zunger, and M. L. Cohen, J. Phys. C **12**, 4409 (1979).
[41] N. Troullier and J. L. Martins, Phys. Rev. B **43**, 1993 (1991).
[42] S. Ismail-Beigi, Phys. Rev. B **73**, 233103 (2006).
[43] L. X. Benedict, C. D. Spataru, and S. G. Louie, Phys. Rev. B **66**, 085116 (2002).
[44] S. Logothetidis and J. Petalas, J. App. Phys. **80**, 1768 (1996).
[45] According to our first-principles calculations (unpublished) on the dielectric function $\varepsilon_{\rm SiC}(q,\omega)$ of 3C-SiC, showing dielectric responses very similar to 6H-SiC (Ref. 44) used in the experiments, $\varepsilon_{\rm SiC}(q,\omega)$ can be well represented by the optical dielectric constant in an energy window $|\omega| < \Delta\omega = 2.5$ eV considered here, and the corresponding wavevector window $|q| < \hbar\Delta\omega/v_{\rm F} = 0.4$ Å^{-1}, with less than 10 % errors, except when the electron wavevector is close to the van Hove singularity.
[46] K. Bolotin *et al.*, Solid State Commun. **146**, 351 (2008).
[47] X. Du, I. Skachko, A. Barker, and E. Y. Andrei, Nature Nanotech. **3**, 491 (2008).
[48] B. Wunsch, T. Stauber, F. Sols, and F. Guinea, New J. Phys. **8**, 318 (2006).

[49] E. H. Hwang and S. D. Sarma, Phys. Rev. B **75**, 205418 (2007).
[50] A. Grüneis *et al.*, Phys. Rev. Lett. **100**, 037601 (2008).
[51] For example, see Refs. 52 and 53 which present calculated electron linewidths for sodium arising from the e-e and the e-ph interactions, respectively.
[52] J. S. Dolado *et al.*, Phys. Rev. B **64**, 195128 (2001).
[53] G. Grimvall, Phys. kondens. Materie **6**, 15 (1967).
[54] We used the scaling relations given in Refs. 16, 17, 18 to account for the difference between the experimental doping level ($E_{\rm D} = -0.87$ eV) and the one considered here ($E_{\rm D} = -1.0$ eV).
[55] A. Canning *et al.*, computer code PARATEC, 2008, http://www.nersc.gov/projects/paratec/.
[56] J. Deslippe *et al.*, computer code BerkeleyGW, 2008.
[57] S. Baroni *et al.*, computer code Quantum-Espresso, 2006, http://www.quantum-espresso.org.
[58] A. Mostofi *et al.*, computer code Wannier90, 2007, http://www.wannier.org.